

Understanding Decreases in Land Relative Humidity with Global Warming: Conceptual Model and GCM Simulations

MICHAEL P. BYRNE

ETH Zürich, Zurich, Switzerland

PAUL A. O'GORMAN

Massachusetts Institute of Technology, Cambridge, Massachusetts

(Manuscript received 1 May 2016, in final form 11 August 2016)

ABSTRACT

Climate models simulate a strong land–ocean contrast in the response of near-surface relative humidity to global warming; relative humidity tends to increase slightly over oceans but decrease substantially over land. Surface energy balance arguments have been used to understand the response over ocean but are difficult to apply over more complex land surfaces. Here, a conceptual box model is introduced, involving atmospheric moisture transport between the land and ocean and surface evapotranspiration, to investigate the decreases in land relative humidity as the climate warms. The box model is applied to simulations with idealized and full-complexity (CMIP5) general circulation models, and it is found to capture many of the features of the simulated changes in land humidity. The simplest version of the box model gives equal fractional increases in specific humidity over land and ocean. This relationship implies a decrease in land relative humidity given the greater warming over land than ocean and modest changes in ocean relative humidity, consistent with a mechanism proposed previously. When evapotranspiration is included, it is found to be of secondary importance compared to ocean moisture transport for the increase in land specific humidity, but it plays an important role for the decrease in land relative humidity. For the case of a moisture forcing over land, such as from stomatal closure, the response of land relative humidity is strongly amplified by the induced change in land surface–air temperature, and this amplification is quantified using a theory for the link between land and ocean temperatures.

1. Introduction

Observations and climate-model simulations show a pronounced land–ocean warming contrast in response to a positive radiative forcing, with land temperatures increasing more than ocean temperatures (Manabe et al. 1991; Sutton et al. 2007; Byrne and O'Gorman 2013a). A land–ocean contrast is also found for the response of near-surface relative humidity in climate-model simulations, with small increases in relative humidity over ocean and larger decreases in relative humidity over continents (O'Gorman and Muller 2010; Lainé et al. 2014; Fu and Feng 2014). This land–ocean contrast in changes in relative humidity is clearly evident in Fig. 1 for simulations from phase 5 of the Coupled Model

Intercomparison Project (CMIP5) that will be discussed in detail in sections 3 and 4. However, the long-term observational trends in near-surface relative humidity are not yet clear. Based on observations over 1975–2005, Dai (2006) found a decreasing trend in surface relative humidity over ocean but no significant trend over land. Willett et al. (2008) also found a negative trend over ocean and no significant trend over land for a similar time period, but they identified a bias in the data prior to 1982 that may cause the apparent negative trend over ocean. Later studies have found a sharp decrease in land relative humidity since 2000 (Simmons et al. 2010; Willett et al. 2014, 2015), but the long-term trend remains insignificant (Willett et al. 2014).

Changes in land relative humidity are important for the land–ocean warming contrast (Byrne and O'Gorman 2013a,b) and for modulating changes in precipitation over land under global warming (Chadwick et al. 2013; Byrne and O'Gorman 2015), and they may affect projected

Corresponding author address: Michael P. Byrne, ETH Zürich, Sonneggstrasse 5, 8092 Zurich, Switzerland.
E-mail: michael.byrne@erdw.ethz.ch

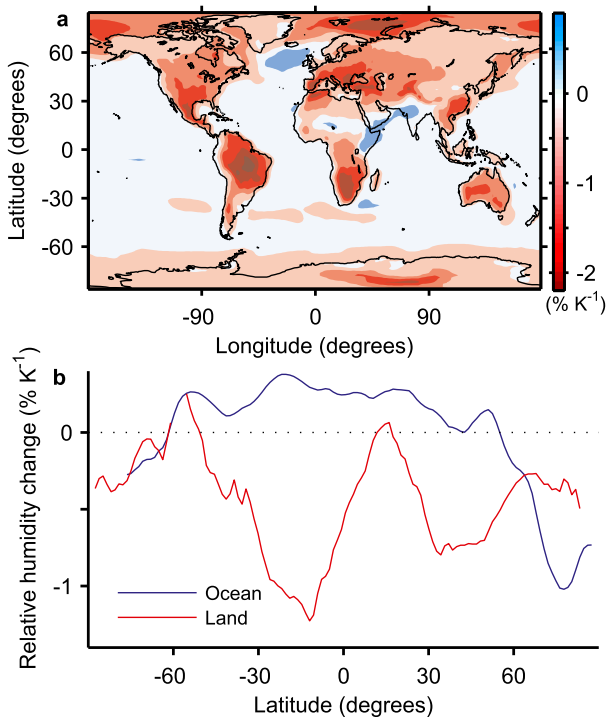


FIG. 1. (a),(b) Multimodel-mean changes in surface-air relative humidity between the historical (1976–2005) and RCP8.5 (2070–99) simulations of CMIP5, normalized by the global- and multimodel-mean surface-air temperature changes. For (b), the zonal averages over all ocean (blue) and land (red) grid points are shown at each latitude. Note that the changes in relative humidity at high latitudes are different from those shown in Fig. 1b of Byrne and O’Gorman (2013b) because Byrne and O’Gorman (2013b) adjusted the relative humidities to be always with respect to liquid water.

increases in heat stress (e.g., Sherwood and Huber 2010). Despite this importance, a clear understanding of what controls land relative humidity is lacking. Here, we introduce a conceptual model based on boundary layer moisture balance to analyze changes in land relative humidity, and we apply this model to idealized and full-complexity general circulation model (GCM) simulations.

We first review the energy balance argument for the small increase in relative humidity over ocean (Held and Soden 2000; Schneider et al. 2010) and why it does not apply over land. Ocean evaporation is strongly influenced by the degree of subsaturation of near-surface air, and changes in ocean relative humidity with warming may be estimated from the changes in evaporation using the bulk formula for evaporation, provided that the air–surface temperature disequilibrium (the difference between the surface-air and surface-skin temperatures) and changes in the exchange coefficient and surface winds are negligible. Schneider et al. (2010) used this approach, together with an energetic estimate for

changes in evaporation, to yield an increase in ocean relative humidity with warming of order $1\% \text{ K}^{-1}$ (here and throughout this paper, relative humidity changes are expressed as absolute rather than fractional changes). The simulated increases in relative humidity over ocean are generally smaller (Fig. 1), indicating that effects such as changes in surface winds must also play a role (e.g., Richter and Xie 2008).

This approach to understanding the increases in ocean relative humidity under warming relies on there being a simple energetic estimate for changes in evaporation and these evaporation changes being easily related to changes in temperature and surface-air relative humidity. These two conditions are generally not valid over land, where the moisture supply for evapotranspiration is limited and varies greatly across continents (De Jeu et al. 2008). The spatially inhomogeneous response of soil moisture to global warming, in addition to changes in land use and changes in stomatal conductance under elevated CO_2 concentrations (e.g., Sellers et al. 1996; Piao et al. 2007; Cao et al. 2010; Andrews et al. 2011; Cronin 2013), leads to land evapotranspiration changes with substantial spatial structure (Lainé et al. 2014), and the near-surface relative humidity is merely one of many factors influencing evapotranspiration changes.

To understand the simulated decreases in land relative humidity under global warming, we take a different approach following previous authors (e.g., Rowell and Jones 2006) who have discussed how the land boundary layer humidity is influenced by the moisture transport from the ocean. Under global warming, as continents warm more rapidly than oceans, the rate of increase of the moisture transport from ocean to land cannot keep pace with the faster increase in saturation specific humidity over land, implying a drop in land relative humidity (Simmons et al. 2010; O’Gorman and Muller 2010; Sherwood and Fu 2014). This explanation is attractive because it relies on robust features of the global warming response—namely, the small changes in relative humidity over ocean and the stronger surface warming over land. Indeed, the most recent Intergovernmental Panel on Climate Change (IPCC) report cites this argument to explain both observed and projected land relative humidity decreases with warming (Collins et al. 2013, section 12.4.5.1). However, this explanation has not been investigated quantitatively using either observations or climate models. Thus, it not clear to what extent changes in land relative humidity can be understood as a simple consequence of the land–ocean warming contrast and changes in moisture transport from ocean to land. Indeed, changes in evapotranspiration resulting from soil moisture decreases (Berg et al. 2016) and stomatal closure (Cao et al. 2010) have been

shown to strongly influence land relative humidity, though such effects are not considered in the simple argument outlined above.

Changes in evapotranspiration may affect relative humidity through induced changes in surface-air temperature as well as through changes in the moisture content of the air. Previous studies have shown that soil drying or decreases in stomatal conductance lead to an increase in surface temperature (e.g., Sellers et al. 1996; Seneviratne et al. 2010; Cao et al. 2010; Andrews et al. 2011; Seneviratne et al. 2013), and this is typically argued to be a result of decreased evaporative cooling of the land surface. But it is difficult to make a quantitative theory for the associated increase in temperature from the surface energy budget because the surface energy fluxes depend on multiple factors over land, and the effect of increased surface sensible heat flux on surface-air temperature cannot be estimated without taking into account atmospheric processes such as convection. The changes in the land surface-air temperature may be instead related directly to changes in surface humidity under climate change by using the fact that atmospheric processes constrain the surface-air equivalent potential temperature (Byrne and O'Gorman 2013a,b). In particular, changes in surface-air temperature and relative humidity combine to give approximately equal increases in equivalent potential temperature over land and ocean. This link between land and ocean is a result of atmospheric dynamical constraints on vertical and horizontal temperature gradients in the atmosphere (see also Joshi et al. 2008) as expressed through the equivalent potential temperature, which is a conserved variable for moist adiabatic processes. Here we use this dynamical constraint to better understand the feedback over land between decreases in relative humidity and increases in surface-air temperature. This temperature-relative humidity feedback is distinct from soil moisture-temperature or soil moisture-precipitation feedbacks that may also be operating (e.g., Seneviratne et al. 2010). We also use the dynamical constraint to estimate the amplification of the relative humidity response to a moisture forcing over land by the induced change in land temperature for the case with ocean temperature and humidity held fixed.

We begin by deriving a conceptual box model for the moisture balance of the land boundary layer (section 2). We apply the box model to idealized GCM and CMIP5 simulations, using first a simplified ocean-influence version of the box model (section 3) and then taking into account evapotranspiration (section 4). We then discuss the role of temperature changes for the response of land relative humidity under climate change (section 5), before summarizing our results (section 6).

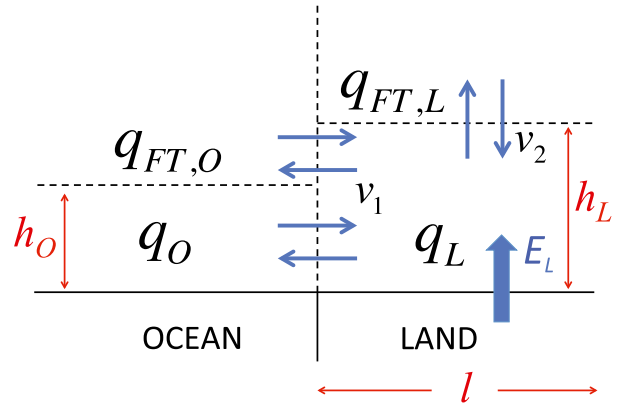


FIG. 2. Schematic diagram of processes involved in the moisture budget of the boundary layer above a land surface [see text and (1) for definitions of the various quantities].

2. Box model of the boundary layer moisture balance over land

Several previous studies have used idealized models to study land-atmosphere interactions (e.g., Brubaker and Entekhabi 1995; Betts 2000; Joshi et al. 2008). The box model used here is of the moisture balance of the atmospheric boundary layer above land (see schematic; Fig. 2). The specific humidity of the land boundary layer is assumed to be determined by three processes: (i) horizontal mixing with the boundary layer and free troposphere over ocean (e.g., via mean-wind advection and diurnal sea breeze), (ii) vertical mixing with the free troposphere over land (via large-scale vertical motion, turbulent entrainment, and shallow and deep convection), and (iii) evapotranspiration. For simplicity, the box model is taken to represent a time average over the diurnal cycle in the boundary layer (see discussion in Betts 2000), and the land boundary layer is assumed to be deeper than the ocean boundary layer. A control-volume analysis for the land boundary layer is then performed, and the time evolution of the average specific humidity in the land boundary layer, q_L , is written as follows:

$$lh_L \frac{dq_L}{dt} = h_O v_1 (q_O - q_L) + (h_L - h_O) v_1 (q_{FT,O} - q_L) + l v_2 (q_{FT,L} - q_L) + \frac{l}{\rho_a} E_L, \quad (1)$$

where l is the horizontal length scale of the land, h_L and h_O are the depths of the boundary layers over land and ocean, respectively; v_1 and v_2 are horizontal and vertical mixing velocities, respectively; q_O is the average specific humidity of the ocean boundary layer; $q_{FT,L}$ and $q_{FT,O}$ are the specific humidities of the free troposphere immediately above the land and ocean boundary layers,

respectively; ρ_a is the density of air; and E_L is the evapotranspiration from the land surface. For simplicity, we further assume that the free-tropospheric specific humidities over land and ocean are proportional to the respective boundary layer specific humidities; that is, $q_{FT,L} = \lambda_L q_L$ and $q_{FT,O} = \lambda_O q_O$, where λ_L and λ_O are the constants of proportionality. (Alternatively, the need to specify the vertical structure of specific humidity over land may be avoided by assuming that the free-tropospheric specific humidities over land and ocean are approximately equal for levels above the land boundary layer.)

For convenience, we define $\tau_1 = l/v_1$ and $\tau_2 = h_L/v_2$ as horizontal and vertical mixing time scales, respectively. Taking the steady-state limit of (1) gives the following:

$$q_L = \frac{[h_O + \lambda_O(h_L - h_O)]\tau_2}{h_L[\tau_1(1 - \lambda_L) + \tau_2]} q_O + \frac{\tau_1\tau_2}{\rho_a h_L[\tau_1(1 - \lambda_L) + \tau_2]} E_L, \quad (2)$$

or

$$q_L = \gamma q_O + q_E, \quad (3)$$

where we have defined the parameter $\gamma = [h_O + \lambda_O(h_L - h_O)]\tau_2 / \{h_L[\tau_1(1 - \lambda_L) + \tau_2]\}$ to quantify the influence of ocean specific humidity on land specific humidity and where $q_E = \tau_1\tau_2 E_L / \{\rho_a h_L[\tau_1(1 - \lambda_L) + \tau_2]\}$ represents the influence of evapotranspiration on land specific humidity. The parameter γ depends on the strengths of the horizontal and vertical mixing processes in the land boundary layer, the boundary layer depths, and the vertical structure of specific humidity over land and ocean. The contribution of evapotranspiration, q_E , is a function of the evapotranspiration rate, the height of the land boundary layer, and other parameters (e.g., evapotranspiration has a weaker influence on land specific humidity in a deeper boundary layer). This box model could be extended in a number of ways, such as by including the diurnal cycle or the source of water vapor due to reevaporation of precipitation.

3. Ocean-influence box model

For the simplest version of our box model, the ‘‘ocean-influence box model,’’ we assume that the influence of evapotranspiration on the boundary layer moisture balance over land is negligible. Setting $E_L = 0$ in (3), we find that

$$q_L = \gamma q_O. \quad (4)$$

Assuming negligible changes in γ , we can write the following:

$$\delta q_L = \gamma \delta q_O, \quad (5)$$

where δ denotes the change in climate. Note that the assumption of constant γ under climate change may hold even if there are changes in the mixing time scales τ_1 and τ_2 . For example, if the overall tropical circulation and convective mass fluxes slow down with climate warming (e.g., Held and Soden 2006; Vecchi and Soden 2007) such that both mixing time scales increase by the same factor, then this will not cause γ to change.

Thus, the ocean-influence box model is consistent with a straightforward hypothesis—that the ratio of land to ocean specific humidity remains approximately constant as the climate changes or, equivalently, that fractional changes in specific humidity over land and ocean are equal:

$$\frac{\delta q_L}{q_L} = \frac{\delta q_O}{q_O}. \quad (6)$$

This result has been derived independently by Chadwick et al. (2016) using a conceptual model based on a Lagrangian analysis of air masses.

In contrast to the fractional changes in specific humidity, fractional changes in saturation specific humidity depend on the local temperature change and will be bigger over land than ocean because of the land–ocean warming contrast (e.g., Sutton et al. 2007). Using (6), and approximating relative humidity as $H = q/q^*$, where q^* is the saturation specific humidity, we express fractional changes in land relative humidity as follows:

$$\begin{aligned} \frac{\delta H_L}{H_L} &= \frac{\delta H_O}{H_O} + \frac{\delta q_O^*}{q_O^*} - \frac{\delta q_L^*}{q_L^*} \\ &= \frac{\delta H_O}{H_O} - \alpha_q (\delta T_L - \delta T_O), \end{aligned} \quad (7)$$

where δT_L and δT_O are the changes in surface air temperature over land and ocean, respectively, and where we have assumed that the saturation specific humidity increases at a fractional rate of $\alpha_q = 0.06 \text{ K}^{-1}$ and that higher-order terms in the changes are negligible. It is clear from (7) that if land warms more than ocean and ocean relative humidity does not change greatly, then the land relative humidity will decrease.

The derivation of the ocean-influence box model given above entirely neglects the influence of evapotranspiration. However, the same results would also follow (with a different definition of γ) if the influence of evapotranspiration on land specific humidity q_E is not neglected but is instead assumed to scale with land specific humidity. Note that q_E may scale with land specific humidity even though the evapotranspiration

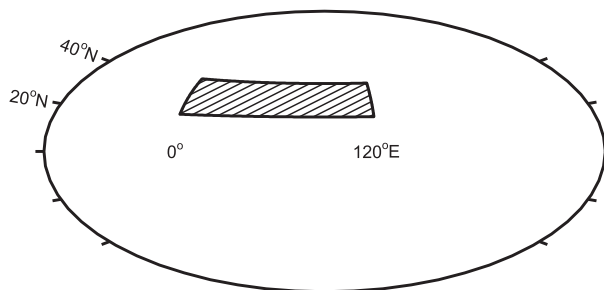


FIG. 3. Continental configuration in the idealized GCM simulations. A subtropical continent spans 20° to 40°N and 0° to 120°E, with a slab ocean elsewhere.

rate is not expected to scale with land specific humidity. In particular, q_E also depends on $\tau_1\tau_2/[\tau_1(1-\lambda_L) + \tau_2]$, and this would be expected to change under a slowdown of the circulation even if both τ_1 and τ_2 increase by the same factor.

We next assess the applicability of this ocean-influence box model result to idealized and comprehensive GCM simulations. We use (5) to estimate the change in land relative humidity under climate change given the changes in land temperature and ocean specific humidity and calculating γ as the ratio of land to ocean specific humidities in the control climate.

a. Application of ocean-influence box model to idealized GCM simulations

The ocean-influence box model is first applied to idealized GCM simulations over a wide range of climates. The idealized GCM does not simulate several features of the climate system (e.g., the seasonal cycle, ocean dynamics, and stomatal effects). However, this reduced-complexity approach and the wide range of climates simulated allow us to systematically investigate land relative humidity in a controlled way and help to guide and interpret our subsequent analysis of more complex CMIP5 simulations.

The idealized GCM is similar to that of Frierson et al. (2006) and Frierson (2007), with specific details as in O’Gorman and Schneider (2008) and Byrne and O’Gorman (2013a). It is based on a spectral version of the GFDL dynamical core, with a two-stream gray radiation scheme, no cloud or water vapor radiative feedbacks, and the simplified moist convection scheme of Frierson (2007). The simulations have a subtropical continent spanning 20° to 40°N and 0° to 120°E, with a slab ocean elsewhere (Fig. 3). The land surface hydrology is simulated using a bucket model (Manabe 1969). According to the bucket model, evapotranspiration is a simple function of soil moisture and the potential evapotranspiration (i.e., the evapotranspiration for a

saturated land surface), with the soil moisture evolving according to the local balance of precipitation and evapotranspiration [see Byrne and O’Gorman (2013a) for a full description of the bucket model employed here]. All other land surface properties are identical to those of the slab ocean. We vary the climate over a wide range of global-mean surface-air temperatures (between 260 and 317 K) by changing the longwave optical thickness, which is analogous to varying the concentrations of CO₂ and other greenhouse gases. The longwave optical thickness is specified by $\tau = \alpha\tau_{\text{ref}}$, where τ_{ref} is a reference optical thickness distribution, and we analyze simulations with 10 different values of the parameter α .¹ We present results based on time averages over 4000 days.

When applying the box model to the simulations, we assume that the average specific humidity in the land boundary layer is a fixed fraction of the surface-air specific humidity² and then use the surface-air specific humidities to represent the boundary layer. In the case of the idealized GCM, surface-air quantities are taken to be those of the lowest atmospheric level, $\sigma = 0.989$, where $\sigma = p/p_s$, and p and p_s are the pressure and surface pressure, respectively. Land values are averaged (with area weighting) over the entire subtropical continent, and the ocean averages are taken over neighboring ocean at the same latitudes—that is, from 20° to 40°N and 120° to 360°E.³

To apply the ocean-influence box model (5), we calculate the γ parameter at each land grid point by taking the ratio of the land specific humidity at that grid point to the zonal-mean ocean specific humidity at that latitude. We calculate γ for each simulation (except the warmest). We then estimate the change in surface-air land specific humidity between pairs of nearest-neighbor simulations as a function of γ and the changes in ocean specific humidity, where γ is set to its value in the colder of the two simulations and assumed to be constant as the climate changes.

¹ Simulations are performed with the following α values: 0.2, 0.4, 0.7, 1.0, 1.5, 2.0, 3.0, 4.0, 5.0, and 6.0.

² This assumption holds approximately in the idealized simulations over land and ocean, although it is less accurate in the coldest simulations over land in which changes in the height of the boundary layer are relatively large (not shown).

³ Our results are almost identical if we calculate ocean averages using the “control” Southern Hemisphere as in Byrne and O’Gorman (2013a) (i.e., ocean values averaged over 20° to 40°S and 0° to 120°E). We choose to average over neighboring ocean in this study because the box model involves advection of moisture from ocean to land, and this naturally suggests averaging over ocean adjacent to the land continent.

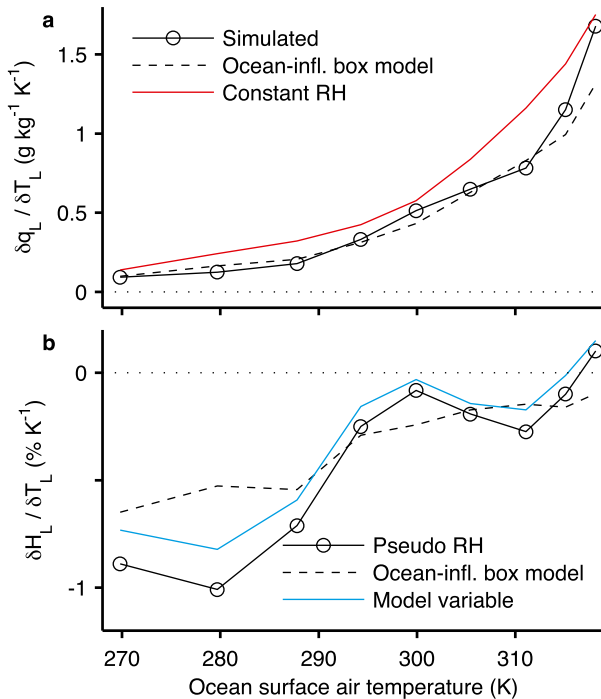


FIG. 4. Changes in (a) surface-air specific humidity and (b) surface-air relative humidity over land between pairs of idealized GCM simulations with a subtropical continent. The humidity changes are normalized by the land surface–air temperature changes. Solid black lines denote the simulated changes and the dashed lines represent the estimated changes using the ocean-influence box model (5). Pseudo relative humidities are shown (see text), but the blue line in (b) shows the change in the mean of the actual relative humidity for comparison. The red line in (a) indicates what the change in surface-air land specific humidity would be if the land pseudo relative humidity did not change (i.e., for each pair of simulations, the land specific humidity change if the land pseudo relative humidity is fixed at its value in the colder simulation).

Land surface–air specific humidity changes between the pairs of idealized GCM simulations, along with the estimates of these changes using (5), are plotted against the midpoint ocean temperature for each pair in Fig. 4. The increases in land specific humidity (Fig. 4a) are smaller than what would occur if land relative humidity remained constant (see the red line in Fig. 4a), implying a decrease in relative humidity with warming. The simulated specific humidity changes are well captured by the ocean-influence box model over the full range of climates (Fig. 4a). The small deviations from the prediction of the ocean-influence box model could be due to the influence of evapotranspiration, changes in circulation patterns, or changes in the ratios λ_L and λ_O of free-tropospheric to surface-air specific humidities, which are assumed to be constant in the box model. The parameters λ_L and λ_O might be expected to increase with warming because the fractional rate of increase in saturation vapor pressure

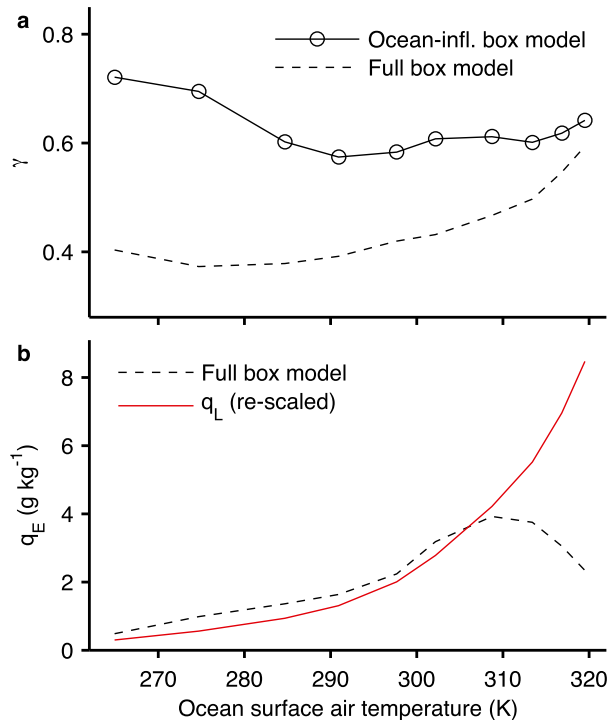


FIG. 5. Parameters for the box models applied to the idealized GCM simulations: (a) The γ parameter for the ocean-influence box model (solid black line) and the full box model (dashed black line). (b) The q_E contribution in the full box model (dashed black line). For comparison, the surface-air land specific humidity is also shown (red line) scaled by a factor of 0.25 so that it roughly matches the magnitude of q_E .

with temperature is higher at the lower temperatures that occur farther up in the atmosphere and because there is enhanced warming aloft at low latitudes in simulations of global warming (e.g., Santer et al. 2005), and such effects could be included in a more complicated box model.

The γ parameter is relatively constant over the wide range of climates simulated (Fig. 5a), consistent with our neglect of changes in γ when deriving (5), with a mean value of 0.63 and minimum and maximum values of 0.57 and 0.72, respectively. Thus, for the subtropical continent in this idealized GCM, land specific humidity is approximately 60% of the neighboring ocean specific humidity.

The box model (5) predicts the changes in mean specific humidity that must be combined with the mean temperatures to estimate the relative humidity changes. However, because of the nonlinearity of the thermodynamic relationship $H(T, p, q)$ between relative humidity, temperature, pressure, and specific humidity, it is not possible to reproduce the mean relative humidity using the mean temperature and mean specific humidity. (For example, the relative humidity may be approximated as the ratio of specific humidity to saturation specific humidity, and it is clear that the mean of this ratio need not be same as the

ratio of the means.) We instead use a pseudo relative humidity, defined in terms of the mean temperature, mean specific humidity, and mean pressure as $H(\bar{T}, \bar{p}, \bar{q})$, where the bars denote time means.⁴ For convenience we will refer to this pseudo relative humidity as the relative humidity, but we also show the mean relative humidity changes for comparison in Figs. 4b and 6b. Although the pseudo relative humidity is not the same as the mean relative humidity, it nonetheless behaves somewhat similarly and is a useful measure of subsaturation.

The box model captures the important features of the relative humidity response including the decreases in relative humidity with warming and the decreasing magnitude of these changes as the climate warms (Fig. 4b). The errors in the estimated changes in relative humidity are larger than for the estimated changes in specific humidity, at least when the sizes of the errors are compared to the sizes of the changes. But this is primarily because the changes in relative humidity are small compared to the fractional changes in specific humidity, which makes them more difficult to estimate accurately.

Given the simplicity of the ocean-influence box model, its ability to describe the behavior of land relative humidity in this idealized GCM is impressive. However, the geometry and surface properties of Earth's landmasses are more varied and complex than the idealized continent considered, and factors such as orography or cloud feedbacks that are not included in the idealized GCM could alter the surface humidity response. Therefore, to investigate the changes in land relative humidity further, we turn to more comprehensive simulations from the CMIP5 archive.

b. Application of ocean-influence box model to CMIP5 simulations

We apply the ocean-influence box model to changes in land surface–air relative humidity between 30-yr time averages in the historical (1976–2005) and RCP8.5 (2070–99) simulations from the CMIP5 archive (Taylor et al. 2012). We analyze 19 models in total,⁵ and in each

case the r11p1 ensemble member is used. As for the idealized GCM analysis, we assume the average boundary layer specific humidity over land is a fixed fraction of the surface-air specific humidity and take surface-air specific humidity to be representative of the boundary layer.

The specific humidities in the box model are identified with the zonal and time mean specific humidities (over land or ocean) for each latitude and for each of the 12 months of the year in the CMIP5 simulations. We calculate γ at each land grid point as the ratio of the local land specific humidity to the zonal-mean ocean specific humidity at that latitude, and we do this for each month of the year in the historical simulations. By computing γ in this way, we are assuming that the horizontal exchange of moisture between land and ocean, described by the box model, is taking place predominantly in the zonal direction. Using the diagnosed γ , and assuming it does not change as the climate warms, changes in mean surface-air specific humidity over land are estimated for each latitude and longitude and for each month of the year using (5) and the changes in zonal-mean ocean specific humidity.

The simulated and estimated annual- and zonal-mean changes in land specific humidity at each latitude are shown in Fig. 6a. The magnitude and latitudinal variations of the specific humidity changes are reasonably well captured by the ocean-influence box model, including the flat region in the Northern Hemisphere midlatitudes. The magnitude of the increases is underestimated at most latitudes, which, as discussed in the case of the idealized GCM simulations, could be partly due to increases in the parameters λ_L and λ_O relating free-tropospheric specific humidities to surface-air specific humidities, but other aspects of the ocean-influence box model such as neglecting the influence of evapotranspiration and the reevaporation of falling precipitation are also likely to play a role. The parameter γ (i.e., the ratio of land and ocean specific humidities) is shown in Fig. 7a. It has a global, annual, and multimodel mean value of 0.75, which is somewhat larger than the value found in the idealized GCM simulations. This is not surprising given that the land in the idealized simulations is a subtropical continent, which is generally drier relative to neighboring oceans than continents at lower or higher latitudes.

Together with the simulated changes in monthly mean surface-air land temperature, the estimated changes in specific humidity are used to estimate the land pseudo relative humidity changes. As for the idealized GCM analysis, it is necessary to compare pseudo relative humidities because of the difficulty in converting time-mean specific humidities estimated by the box model to

⁴ When evaluating pseudo relative humidity for the idealized GCM, we use a simplified form of the Clausius–Clapeyron relation (consistent with the idealized GCM) that considers only the vapor–liquid phase transition when computing the saturation vapor pressure [see Eq. (4) of O'Gorman and Schneider 2008].

⁵ The CMIP5 models considered are ACCESS1.0, ACCESS1.3, BCC_CSM1.1, BCC_CSM1.1(m), BNU-ESM, CanESM2, CNRM-CM5, CSIRO Mk3.6.0, GFDL CM3, GFDL-ESM2M, INMCM4, IPSL-CM5A-LR, IPSL-CM5A-MR, IPSL-CM5B-LR, MIROC-ESM, MIROC-ESM-CHEM, MIROC5, MRI-CGCM3, and NorESM1-M. The variables used in this paper have the following names in the CMIP5 archive: evaporation (evspsbl), surface-air specific humidity (huss), surface-air temperature (tas), and surface-air relative humidity (hurs).

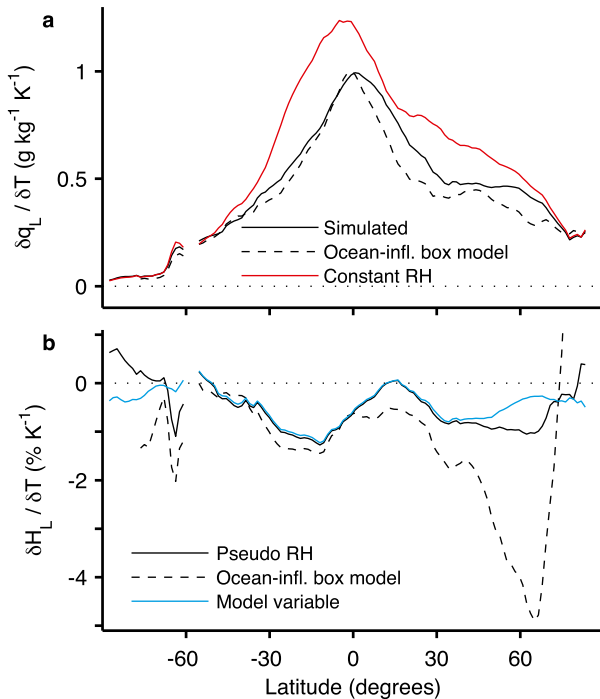


FIG. 6. Multimodel-mean changes between the historical and RCP8.5 simulations in zonal and time mean (a) surface-air land specific humidity and (b) surface-air land relative humidity. The changes are normalized by the global-mean surface-air temperature change prior to taking the multimodel mean. Solid black lines denote the simulated changes and dashed lines denote the estimated changes using the box model (5). For (a), the red line indicates the change in surface-air land specific humidity for constant land pseudo relative humidity (i.e., for land pseudo relative humidities fixed at the values in the historical simulations). Pseudo relative humidities are shown, but the blue line in (b) shows the simulated mean changes for the relative humidity variable outputted by the models for comparison.

relative humidities. The use of pseudo relative humidities also avoids the complication that different climate models use different saturation vapor pressure formulations.⁶ The changes in pseudo relative humidity are calculated for each month of the year before taking the annual mean for both the simulated changes and the changes estimated by the box model. The changes in pseudo relative humidity and model-outputted relative humidity are very similar at lower latitudes but more different at higher latitudes (cf. blue and black solid lines

⁶ CMIP5 models use a variety of forms for the dependence of saturation vapor pressure on temperature (including the issue of how ice is treated), but documentation regarding the specific form used by a given model is not readily available. We use a relatively simple expression for the saturation vapor pressure [see Eq. (10) of Bolton 1980] to calculate the pseudo relative humidities for all the models.

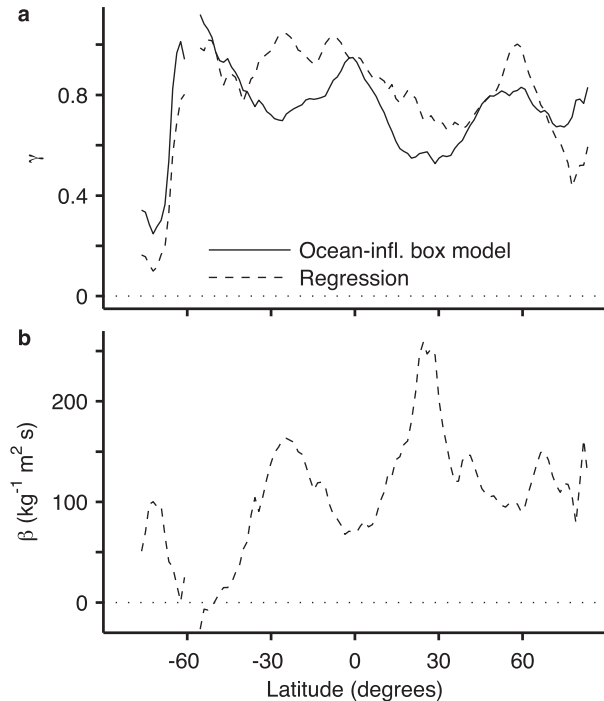


FIG. 7. Parameters in the ocean-influence box model and regression approach for the CMIP5 simulations: (a) γ parameter for the ocean-influence box model in the multimodel mean (solid black line) and for the regression approach including evapotranspiration (dashed black line) and (b) the regression coefficient β . For the ocean-influence box model, γ is evaluated based on the historical simulations. For the regression approach, γ and β are evaluated based on (9) across the different models.

in Fig. 6b), where the differing computations of saturation vapor pressure over ice in the various models become important and there is larger temporal variability.

The simulated changes in (pseudo) land relative humidity are quite well described by the ocean-influence box model in the Southern Hemisphere and at lower latitudes (Fig. 6b). However, owing to the general underestimation of the specific humidity increases by the ocean-influence box model (Fig. 6b), the relative humidity decreases are overestimated, with a large discrepancy in the mid- to high latitudes of the Northern Hemisphere. At these latitudes, there is more land than ocean and it is likely that changes in ocean specific humidity have a weak influence on the specific humidity in the interior of large continents or that meridional moisture transports from ocean at other latitudes become more important.

The estimated and simulated rates of change of global-mean land relative humidity (in $\% K^{-1}$) in the various climate models are correlated, with a correlation coefficient of 0.64 (Fig. 8). According to the ocean-influence box model, intermodel differences in the

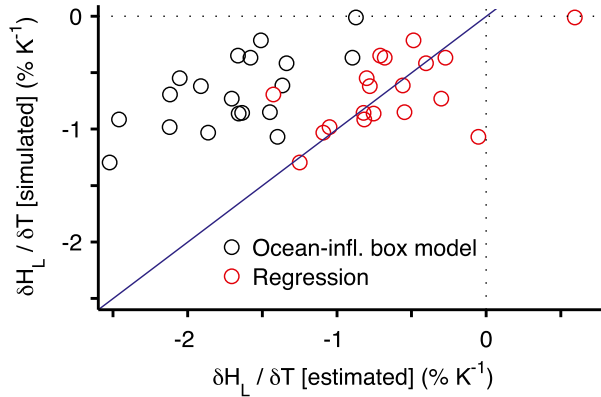


FIG. 8. Simulated global mean changes in (pseudo) land relative humidity vs their estimates from the ocean-influence box model (black circles) and the regression approach that includes evapotranspiration (red circles) for the various CMIP5 models. Both the simulated and estimated changes are normalized by the global-mean surface-air temperature change for each model. The correlation coefficients are 0.64 and 0.56 for the ocean-influence box model and the regression approach, respectively, and the solid line is the one-to-one line.

relative humidity change may be related to the differences in the control-climate land relative humidity, land–ocean warming contrast, and fractional change in ocean relative humidity [see (7)]. Of these factors, we find that the simulated change in land relative humidity is best correlated with the land–ocean warming contrast. The links between changes in temperature and relative humidity are discussed in more detail in section 5.

4. Influence of evapotranspiration

The ocean-influence box model captures much (but not all) of the behavior in vastly more complex GCMs. However, the moisture balance of the land boundary layer is also affected by evapotranspiration, and changes in land surface properties, such as soil moisture or stomatal conductance that are exogenous to the box model, can affect evapotranspiration in the absence of any changes in the overlying atmosphere. For example, changes in stomatal conductance under elevated CO_2 conditions have been shown to reduce both evapotranspiration and land relative humidity without changes in ocean humidity (Andrews et al. 2011).

We turn to the full box model (3), which includes the effects of evapotranspiration. We assume once more that changes in γ are negligible, such that

$$\delta q_L = \gamma \delta q_O + \delta q_E. \quad (8)$$

There are two terms contributing to changes in q_L in (8): the term arising from changes in ocean specific humidity,

$\gamma \delta q_O$, and an additional land evapotranspiration term, δq_E . We next assess their relative importance in controlling changes in land humidity in the idealized GCM and CMIP5 simulations.

a. Application of full box model to idealized GCM simulations

We first examine the idealized GCM simulations with a subtropical continent. In contrast to the ocean-influence box model (5), for which the single parameter γ could be easily estimated in the control simulation in each case, the full model in (8) has two parameters to be estimated, γ and q_E . To estimate these parameters, we perform an additional set of simulations with the same longwave optical thicknesses as in the 10 simulations described previously but with the evapotranspiration set to zero over land. Specifying the land evapotranspiration in this way is equivalent to drying out the soil. (Note that the change in evapotranspiration affects both the humidity of the atmosphere and the surface energy balance.) Using these additional simulations with $E_L = 0$, we can estimate γ for each land grid point and for each climate using (3): $\gamma = q_{L,E_L=0}/q_{O,E_L=0}$, where the ocean specific humidity is zonally averaged at the latitude of the given land grid point. The γ values obtained are smaller than those calculated from the control climate for the ocean-influence box model (Fig. 5a) because the contribution of evapotranspiration to the land specific humidity is now also taken into account. We use these γ values to estimate q_E for the original simulations with dynamic land surface hydrology: $q_E = q_L - \gamma q_O$. The values of q_E increase with warming except in hot climates (Fig. 5b). Interestingly, the influence of evapotranspiration on land specific humidity, as measured by q_E , roughly scales with the land specific humidity except in hot climates (cf. the dashed black and solid red lines in Fig. 5b), and this helps to explain why the ocean-influence box model is accurate even though evapotranspiration affects land specific humidity.

We then estimate the changes in land specific humidity between pairs of nearest-neighbor simulations from (8), which assumes that γ is constant as the climate changes. We calculate changes in the influence of evapotranspiration δq_E using the values of q_E diagnosed for each simulation as described above. The simulated and estimated changes in surface-air land specific humidity, along with the contributions due to changes in ocean specific humidity and land evapotranspiration, are shown in Fig. 9a. The full box model captures the behavior of the land specific humidity changes as a function of temperature, although it is less accurate in hot climates because of increases in γ with warming in these climates (Fig. 5a). The contribution from ocean specific

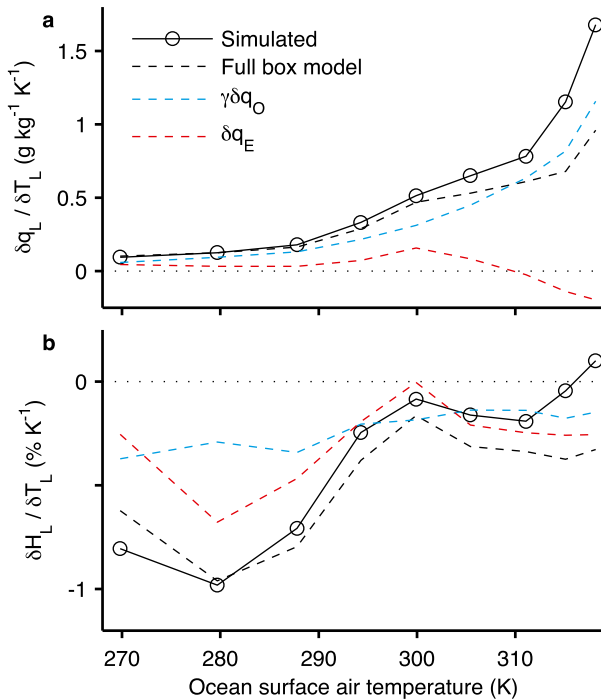


FIG. 9. As in Fig. 4, but here showing estimates of the surface-air (a) specific humidity changes and (b) relative humidity changes from the full box model (8). The contributions due to ocean specific humidity changes (blue dashed lines) and evapotranspiration changes (red dashed lines) are also shown. The contributions to changes in relative humidity are calculated using (A3). Pseudo relative humidities are shown in this figure (the changes in actual relative humidity are shown by the blue line in Fig. 4b).

humidity changes $\gamma\delta q_O$ is larger than the contribution from land evapotranspiration δq_E for all climates (Fig. 9a). The changes in simulated land (pseudo) relative humidity are also well captured by the full box model (Fig. 9b).

Because relative humidity depends on temperature as well as specific humidity, there is no unique way to use the box model result (8) to decompose changes in land relative humidity into contributions due to ocean specific humidity and land evapotranspiration. However, a decomposition derived in appendix A [(A3)] has several desirable properties. According to the decomposition, the contributions to the change in land relative humidity from evapotranspiration and ocean specific humidity are weighted according to their contribution to land specific humidity in the control climate. The change in ocean specific humidity leads to a decrease in land relative humidity if the fractional increase in ocean specific humidity is less than the fractional increase in saturation specific humidity over land. Similarly, evapotranspiration contributes to a decrease in land relative humidity if the fractional increase in q_E is less than the fractional

increase in saturation specific humidity over land. (Note that the fractional change in q_E is generally different from the fractional change in evapotranspiration.)

Using this decomposition of the change in land relative humidity, we find that the land evapotranspiration contribution is of comparable importance to the ocean specific humidity contribution for the idealized GCM simulations (Fig. 9b). By contrast, we found that the contribution of ocean specific humidity was more important than land evapotranspiration when land specific humidity changes were considered. The discrepancy arises because, according to the decomposition [(A3)], it is not the magnitude of a particular contribution to the change in specific humidity that matters for its contribution to the change in relative humidity, but rather how its fractional changes compare to the fractional changes in saturation specific humidity and how much it contributes to the land specific humidity in the control climate.

b. Influence of evapotranspiration in CMIP5 simulations

We now investigate how land evapotranspiration contributes to specific humidity changes in the CMIP5 simulations. We need to estimate both γ and q_E for the full box model, but there are no CMIP5 simulations analogous to the zero-evapotranspiration simulations with the idealized GCM described above. Instead, we estimate the influence of evapotranspiration and ocean specific humidity on land specific humidity using a multiple linear regression approach based on the inter-model scatter across the CMIP5 models. We use the following regression relationship:

$$\delta q_L = \gamma\delta q_O + \beta\delta E_L + \zeta, \quad (9)$$

which is motivated by the full box model (3), but note that $\beta\delta E_L$ will only equal δq_E if parameters such as τ_1 and τ_2 do not change with climate (changes in these parameters will contribute to the remainder term ζ). The variable δq_O is identified as the zonal and time mean for each latitude and month of the year in each model, whereas δq_L and δE_L are the time mean values at each latitude, longitude, and month of the year. The regression coefficients γ , β , and ζ are then estimated using ordinary least squares regression for each land grid point and month of the year, implying that γ , β , and ζ are assumed to be the same in all models. The zonal and annual means are shown for γ and β in Fig. 7 and for ζ in Fig. 10. The regression coefficient γ has a similar magnitude and latitudinal structure to the γ parameter calculated for the ocean-influence box model (Fig. 7a). The coefficient β is positive at almost all latitudes (Fig. 7b),

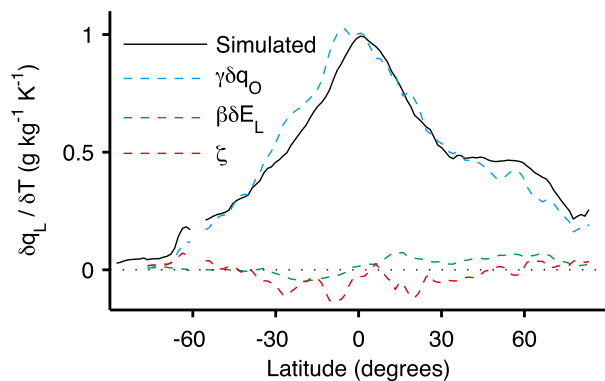


FIG. 10. Multimodel-mean changes in zonal- and time-mean surface-air land specific humidity (solid black line) in the CMIP5 simulations and the contributions to these changes due to ocean specific humidity changes $\gamma\delta q_O$ (blue dashed line), land evapotranspiration changes $\beta\delta E_L$ (green dashed line), and the remainder term ζ (red dashed line) as estimated using the regression relation (9). All quantities are normalized by the global-mean surface-air temperature change.

indicating that enhanced evapotranspiration increases the land specific humidity, while the remainder term ζ (Fig. 10) is negative at most latitudes.

By construction, the regression relationship (9) is exactly satisfied in the multimodel mean. Based on this relationship, the annual-mean contributions to changes in land specific humidity from changes in ocean specific humidity, changes in land evapotranspiration, and the remainder term are shown in Fig. 10. At all latitudes, changes in land specific humidity are dominated by the ocean specific humidity contribution. The contribution due to changes in land evapotranspiration is positive and has its largest values in the Northern Hemisphere where the land fraction is greatest. The global-mean land relative humidity changes estimated using the regression relationship are not as highly correlated with the simulated changes as for the ocean-influence box model (Fig. 8), and this may be because γ variations across the models are not taken into account.

It is not possible to estimate the individual contributions to changes in land relative humidity from ocean specific humidity and evapotranspiration for the CMIP5 simulations, as we did for the idealized GCM simulations. This is because the decomposition of relative humidity changes discussed in appendix A involves the individual contributions to land specific humidity in the control climate, and these are difficult to calculate using a regression approach. However, the results from the idealized GCM simulations suggest that evapotranspiration could be important for the changes in land relative humidity in the CMIP5 simulations, even though it is a second-order influence for changes in land

specific humidity. It would be worthwhile to estimate the land evapotranspiration contribution for full-complexity GCMs by performing simulations with specified land evapotranspiration rates as was done for the idealized GCM in this study.

5. Role of temperature change for the response of land relative humidity to climate change

Throughout this paper, we have calculated changes in land relative humidity by first estimating the specific humidity changes and then combining these estimates with the temperature changes, which we have taken as independently specified. However, changes in land humidity can be expected to lead to changes in surface-air temperature, and this can be quantified through the atmospheric dynamic constraint linking changes in temperature and relative humidity over land and ocean (Byrne and O’Gorman 2013a,b). In the tropics, this constraint is based on weak horizontal gradients of temperature in the free troposphere and convective quasi equilibrium in the vertical. As a result, land temperatures and relative humidities must change in tandem as the climate warms such that the change in surface-air equivalent potential temperature θ_e is approximately the same over land and ocean ($\delta\theta_{e,L} = \delta\theta_{e,O}$). Byrne and O’Gorman (2013a) referred to this constraint as the convective quasi-equilibrium theory of the land–ocean warming contrast, and they also discussed extensions to the extratropics. Here we are not focused on the land–ocean warming contrast and we will simply refer to this constraint as the dynamic constraint on surface-air temperatures and humidities since it follows from atmospheric dynamical processes. By contrast, we will refer to the link between surface-air humidities over land and ocean because of moisture transport between them (as formulated in the box model in this paper) as the moisture constraint ($\delta q_L = \gamma\delta q_O + \delta q_E$). As shown in appendix B, the dynamic constraint and ocean-influence box model may be combined to give first-order estimates of the land–ocean warming contrast and the change in land relative humidity based only on changes in humidity and temperature over ocean and control-climate variables.

A feedback loop is used to conceptualize the interaction between changes in temperature and relative humidity over land and ocean (Fig. 11). As mentioned earlier, this feedback is separate to the soil moisture–temperature and soil moisture–precipitation feedbacks identified in other studies (e.g., Seneviratne et al. 2010). Air over land is drier than air over ocean in the control climate, and as a result the dynamic constraint implies that surface-air temperatures increase more over land than ocean in response to a positive radiative forcing (Byrne and O’Gorman 2013a). The moisture constraint

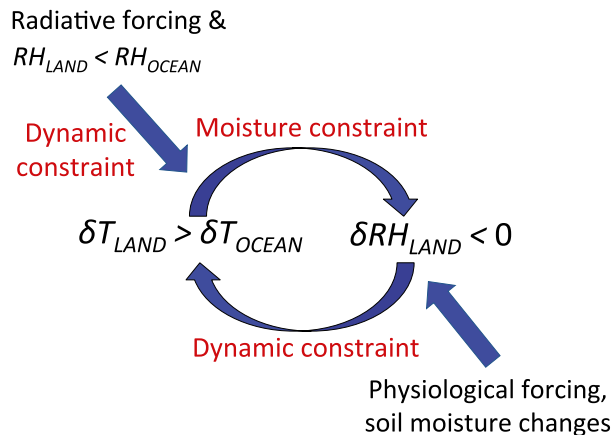


FIG. 11. Schematic diagram describing the feedback between changes in temperature and relative humidity over land and ocean (assuming, for simplicity, that ocean relative humidity remains constant). The “dynamic constraint” arises from atmospheric processes that link temperatures and relative humidities over land and ocean. The “moisture constraint” is due to the limited supply of moisture from the ocean to the land boundary layer.

then implies that the enhanced land warming leads to a land relative humidity decrease because of the limited supply of moisture from the ocean. According to the dynamic constraint, a decrease in land relative humidity enhances the land warming further. The feedback loop can also be entered via a nonradiative forcing that causes a decrease in land specific humidity, such as the physiological forcing from reduced stomatal conductance or a local decrease in soil moisture.

We next assess the amplification of land relative humidity changes by induced changes in temperature for the case in which a moisture forcing (e.g., stomatal closure) alters the specific humidity over land by changing evapotranspiration, while the ocean temperature and humidity are assumed to remain constant. Considering the relative humidity to be a function of specific humidity and temperature and linearizing, we can write the total change in land relative humidity as the sum of contributions from changes in specific humidity at constant temperature (the “forced” component) and changes in temperature at constant specific humidity:

$$\delta H_{L,\text{total}} = \delta H_{L,\text{forced}} + \left. \frac{\partial H_L}{\partial T_L} \right|_{q_L} \delta T_L, \quad (10)$$

where $\left. \frac{\partial H_L}{\partial T_L} \right|_{q_L}$ is the sensitivity of relative humidity to warming at constant specific humidity, and δT_L is the change in land temperature that arises as a result of the change in land humidity.

Because the change in land specific humidity is given in this case, it is simplest to calculate δT_L directly using the dynamic constraint written in terms of specific humidity

rather than following a feedback loop in relative humidity as in Fig. 11. The analysis is also simpler if the dynamic constraint is formulated in terms of moist static energy. Like equivalent potential temperature, moist static energy is conserved for certain moist adiabatic displacements of air, and it is defined as $h = c_p T + L_v q + \phi$, where c_p is the specific heat capacity at constant pressure, L_v is the latent heat of evaporation, and ϕ is the geopotential. Given that the surface geopotential is constant as the climate changes, the dynamic constraint may be expressed as equal changes in surface-air moist enthalpy over land and ocean:

$$c_p \delta T_L + L_v \delta q_L = c_p \delta T_O + L_v \delta q_O. \quad (11)$$

Thus, the assumption of equal changes in moist enthalpy over land and ocean as used previously by Berg et al. (2016) is consistent with the theory of the land–ocean warming contrast used by Byrne and O’Gorman (2013b) when the equivalent potential temperature is replaced by the moist static energy. The expression (11) provides a particularly simple way to think about the response of relative humidity to a moisture forcing over land. A decrease in land specific humidity (due to, e.g., reduced stomatal conductance) requires an increase in land temperature so as to maintain a constant moist enthalpy (assuming no change over ocean). Both the decrease in land specific humidity and the consequent increase in land temperature contribute to a decrease in land relative humidity.

For constant ocean humidity and temperature, (11) gives $\delta T_L = -L_v \delta q_L / c_p$. Approximating $H_L = q_L / q_L^*$, we can also write $\delta H_{L,\text{forced}} = \delta q_L / q_L^*$ and $\left. \frac{\partial H_L}{\partial T_L} \right|_{q_L} = -\alpha_q H_L$, where we have again assumed that saturation specific humidity varies with temperature at a fractional rate of α_q . Substituting these expressions into (10) we find that

$$\delta H_{L,\text{total}} = \delta H_{L,\text{forced}} \left(1 + \frac{\alpha_q L_v q_L}{c_p} \right), \quad (12)$$

which implies that the forced relative humidity change is amplified by a factor of $(1 + \alpha_q L_v q_L / c_p)$ by the induced change in temperature, and this factor is an increasing function of the control-climate specific humidity over land. For a control land relative humidity of 50%, a land surface temperature of 298 K, and taking $\alpha_q = 0.06 \text{ K}^{-1}$, the amplification of the relative humidity change is by a factor of 2.5. For a less arid region with higher humidity, the amplification is even larger (e.g., for the same temperature and a relative humidity of 70% the amplification of the relative humidity change is by a factor of 3). Very similar numerical results are obtained if the dynamic constraint is formulated in terms of equivalent

potential temperature, and the calculation is performed following the feedback loop between temperature and relative humidity as in Fig. 11.

Thus, temperature changes strongly amplify changes in relative humidity due to moisture forcings over land (e.g., from changes in stomatal conductance or soil moisture). Indeed, more than half of the total change in relative humidity in this case comes from the change in temperature rather than the change in specific humidity, and this holds true for control land specific humidities above $c_p/(\alpha_q L_v) = 6.7 \text{ g kg}^{-1}$ according to (12).

Equation (12) can also be used to quantify the relative influence of a land moisture forcing on relative humidity versus specific humidity. The ratio of the fractional change in relative humidity, $\delta H_L/H_L$, to the fractional change in specific humidity, $\delta q_L/q_L$, is given by the factor $(1 + \alpha_q L_v q_L/c_p)$, which is always greater than one. Thus, a land moisture forcing has a greater effect on relative humidity than specific humidity. This is because the moisture forcing and the induced temperature change act in the same direction on relative humidity (unlike for the global warming case). For example, stomatal closure reduces the specific humidity and increases the temperature, both of which reduce the relative humidity.

6. Conclusions

We have introduced a conceptual box model to investigate the response of near-surface land relative humidity to changes in climate. Neglecting the contribution q_E of evapotranspiration to the moisture balance over land (or assuming that q_E scales with land specific humidity), the simplest version of the box model suggests a purely oceanic control on land boundary layer humidity, with equal fractional changes in specific humidity over land and ocean. Together with enhanced warming over land relative to ocean and small changes in ocean relative humidity, this simple box model implies a decrease in land relative humidity as the climate warms, consistent with the mechanism proposed previously for decreases in land relative humidity with global warming (Simmons et al. 2010; O'Gorman and Muller 2010; Sherwood and Fu 2014). The ocean-influence box model captures many features of the specific humidity response in idealized GCM and CMIP5 simulations, supporting the hypothesis of a strong oceanic influence on surface-air specific humidity over land.

The full box model, incorporating evapotranspiration, is applied to the idealized GCM simulations using additional simulations with specified evapotranspiration rates and to the CMIP5 simulations using a linear

regression approach. Compared to moisture transport from the ocean, evapotranspiration has only a secondary influence on the land specific humidity and its changes. However, evapotranspiration does play an important role for the changes in land relative humidity in the idealized GCM simulations according to a decomposition of the relative humidity change that takes the temperature change as given. Thus, although the oceanic influence dominates changes in land specific humidity, in agreement with the prevailing hypothesis, changes in evapotranspiration must also be taken into account for the change in land relative humidity.

The responses of land relative humidity and temperature to climate change are not independent, and their interaction can generally be described by a temperature–relative humidity feedback associated with the dynamic constraint between land and ocean temperatures and humidities and the moisture constraint described in this paper. For the particular case of a moisture forcing over land with ocean temperature and humidity held fixed, we have derived a simple expression for the amplification of the relative humidity change by the induced change in land temperature, and we have given an example in which the amplification is by a factor of 2.5 for a land relative humidity of 50% and a land surface temperature of 298 K. For sufficiently high specific humidity in the control climate, the majority of the change in land relative humidity comes from the induced change in temperature rather than the change in specific humidity. This amplification contributes to the strong influence of reduced stomatal conductance or decreases in soil moisture on land relative humidity found in previous studies (e.g., Cao et al. 2010; Andrews et al. 2011; Berg et al. 2016).

As mentioned in section 1, the pattern of relative humidity changes influences the projected response of the water cycle to climate change. In particular, spatial gradients of fractional changes in surface-air specific humidity $\delta q/q$ contribute a negative tendency to precipitation minus evapotranspiration ($P - E$) over continents as the climate warms (Byrne and O'Gorman 2015). The ocean-influence box model predicts that $\delta q/q$ is spatially uniform, implying no effect of spatial gradients in this quantity on $P - E$ changes over land. However, the CMIP5 simulations do show spatial gradients in $\delta q/q$, and thus a more detailed understanding of the pattern of relative humidity changes is needed for the purpose of understanding changes in $P - E$ over land. On the other hand, the prediction of equal fractional increases in specific humidity over land and ocean may help explain the equal fractional increases in the intensity of precipitation extremes over tropical land and ocean that have previously

been found in climate-model simulations (see Fig. S3 of O’Gorman 2012).

Future work could investigate the controls on the detailed pattern of $\delta q/q$ in order to better understand the $P - E$ response over land. Further investigation of the contribution of evapotranspiration changes to land relative humidity changes in simulations of global warming with comprehensive GCMs would also be valuable. In addition, the influence of other factors on the land relative humidity response to global warming could be investigated. For example, enhanced reevaporation of precipitation due to reduced land relative humidity in a warmer climate would tend to moisten the land boundary layer and dampen the decrease in relative humidity. Finally, it is of interest to determine if the box models discussed here can be adapted for application to shorter-term variability and in particular to the sharp decrease in global-mean land relative humidity that is seen in observations since 2000 (Simmons et al. 2010; Willett et al. 2014, 2015).

Acknowledgments. We thank Alexis Berg, Bill Boos, Sonia Seneviratne, and Bjorn Stevens for helpful discussions. We thank Jack Scheff for pointing out that the moist static energy formulation leads to the particularly simple expression (12). We also thank three anonymous reviewers for their comments and suggestions. We acknowledge the World Climate Research Programme’s Working Group on Coupled Modelling, which is responsible for CMIP, and we thank the climate modeling groups for producing and making available their model output. For CMIP, the U.S. Department of Energy’s Program for Climate Model Diagnosis and Intercomparison provides coordinating support and led development of software infrastructure in partnership with the Global Organization for Earth System Science Portals. We acknowledge support from NSF Grants AGS-1148594 and AGS-1552195.

APPENDIX A

Decomposition of Changes in Land Relative Humidity

In this appendix we derive a decomposition of the changes in land relative humidity into contributions associated with changes in ocean specific humidity and with land evapotranspiration.

We approximate relative humidity as the ratio of specific humidity to saturation specific humidity $H = q/q^*$. We can then write changes in specific humidity as follows:

$$\delta q = H\delta q^* + q^*\delta H + \delta H\delta q^*. \quad (\text{A1})$$

Dividing (A1) by the specific humidity q and rearranging, we can express fractional changes in relative humidity as follows:

$$\frac{\delta H}{H} = \left(\frac{\delta q}{q} - \frac{\delta q^*}{q^*} \right) \frac{q^*}{q^* + \delta q^*}. \quad (\text{A2})$$

Using (8), we relate changes in land specific humidity to changes in ocean specific humidity and changes in evapotranspiration (i.e., $\delta q_L = \gamma\delta q_O + \delta q_E$) and substitute into (A2) to obtain an expression for fractional changes in land relative humidity in terms of an ocean specific humidity contribution and an evapotranspiration contribution:

$$\frac{\delta H_L}{H_L} = \underbrace{\frac{\gamma q_O}{q_L} \left(\frac{\delta q_O}{q_O} - \frac{\delta q_L^*}{q_L^*} \right) \frac{q_L^*}{q_L^* + \delta q_L^*}}_{\gamma\delta q_O \text{ contribution}} + \underbrace{\frac{q_E}{q_L} \left(\frac{\delta q_E}{q_E} - \frac{\delta q_L^*}{q_L^*} \right) \frac{q_L^*}{q_L^* + \delta q_L^*}}_{\delta q_E \text{ contribution}}. \quad (\text{A3})$$

The properties of this decomposition are discussed in section 4a.

APPENDIX B

Estimates of the Land–Ocean Warming Contrast and Land Relative Humidity Changes Based on Combined Dynamic and Moisture Constraints

In this paper, we have estimated the land surface–air relative humidity change by estimating the change in land specific humidity and taking the land temperature change as an input. By contrast, Byrne and O’Gorman (2013b) estimated the land temperature change by assuming changes in equivalent potential temperature were the same over land and ocean (the dynamic constraint) and taking the land relative humidity change as an input. Here, the dynamic and moisture constraints are combined to give simple estimates of the land–ocean warming contrast and land relative humidity changes without prescribing changes in either land temperature or relative humidity.

We use the form of the dynamic constraint in terms of moist static energy that is discussed in section 5. Rearranging (11) and using the moisture constraint from the ocean-influence box model (5), we can estimate the warming amplification factor A , defined as the ratio of land warming to ocean warming (e.g., Byrne and O’Gorman 2013a):

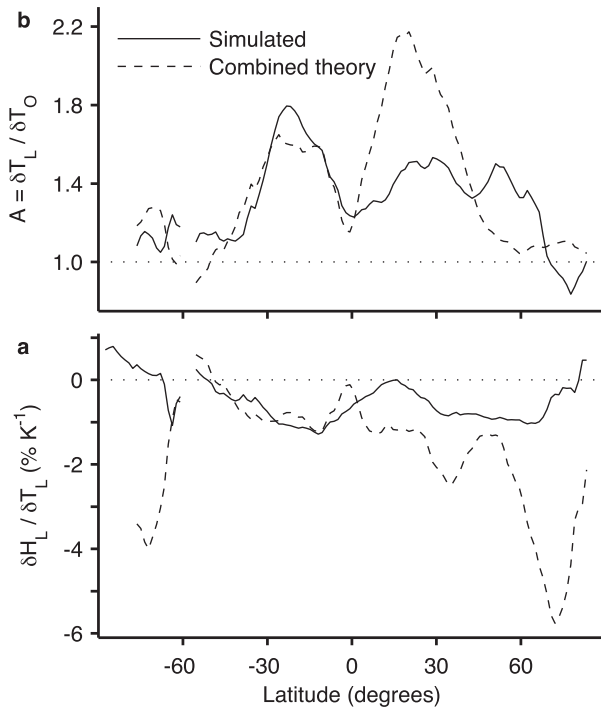


FIG. B1. The CMIP5 multimodel mean (a) land–ocean warming contrast (expressed as an amplification factor) and (b) surface–air land pseudo relative humidity change normalized by the global-mean surface–air temperature change (solid lines) and as estimated by the combined moisture and dynamic constraints (dashed lines). The amplification factor and land relative humidity changes are estimated for each land grid point and for each month of the year before taking the zonal and annual means.

$$A = \frac{\delta T_L}{\delta T_O} = 1 + (1 - \gamma) \frac{L_v}{c_p} \frac{\delta q_O}{\delta T_O}. \quad (\text{B1})$$

The estimated change in land temperature from (B1) may then be combined with the estimated change in land specific humidity from the ocean-influence box model (5) to give an estimate of the change in land relative humidity. Thus, the combination of the dynamic and moisture constraints gives estimates for the changes in land temperature and relative humidity using only control-climate variables and changes in temperature and humidity over ocean.

We apply this combined theory to the CMIP5 simulations and compare the estimated amplification factors and land relative humidity changes to the simulated values (Fig. B1). The amplification factor is well estimated in the Southern Hemisphere (Fig. B1a), but it is substantially overestimated in the northern subtropics. The change in land relative humidity is also well estimated in the Southern Hemisphere except over Antarctica (Fig. B1b) but is less accurate in the Northern Hemisphere where the land fraction is larger and we

expect the moisture constraint derived from the ocean-influence box model to be less valid. The accuracy of the amplification factor estimate is lower than when only the dynamic constraint is used (cf. Fig. 2 of Byrne and O’Gorman 2013b), and this is not surprising given that errors in estimating the land relative humidity using the ocean-influence box model will make a contribution. Nevertheless, given that only changes in ocean quantities are used, the combined theory provides reasonable first-order estimates of the land–ocean warming contrast and land relative humidity changes.

More accurate results could be obtained by combining the dynamic constraint with the full box model for the relative humidity change, which takes account of the influence of evapotranspiration and thus factors such as stomatal closure. Thus, our results are consistent with the conclusion of Berg et al. (2016) that for a given change in moist enthalpy over land, land surface processes modulate the partitioning between changes in temperature and changes in specific humidity, but we note that the ocean influence on land moisture also helps to determine this partitioning.

Although the combined dynamic and moisture constraints give reasonable first-order estimates of the land relative humidity change and the land–ocean warming contrast for the CMIP5 models, they give very inaccurate estimates for the idealized GCM simulations in warm and hot climates (not shown). The reason for this inaccuracy seems to be that the ocean-influence box model predicts the change in land specific humidity or pseudo relative humidity, but the prediction from the dynamic constraint [i.e., the convective quasi-equilibrium theory of the land–ocean warming contrast in Byrne and O’Gorman (2013a)] only works well for the idealized GCM simulations when it is evaluated in terms of the mean relative humidity. This issue highlights the sensitivity of the land–ocean warming contrast to even small differences in the change in land relative humidity.

REFERENCES

- Andrews, T., M. Doutriaux-Boucher, O. Boucher, and P. M. Forster, 2011: A regional and global analysis of carbon dioxide physiological forcing and its impact on climate. *Climate Dyn.*, **36**, 783–792, doi:10.1007/s00382-010-0742-1.
- Berg, A. M., and Coauthors, 2016: Land–atmosphere feedbacks amplify aridity increase over land under global warming. *Nat. Climate Change*, **6**, 869–874, doi:10.1038/nclimate3029.
- Betts, A. K., 2000: Idealized model for equilibrium boundary layer over land. *J. Hydrometeor.*, **1**, 507–523, doi:10.1175/1525-7541(2000)001<0507:IMFEBL>2.0.CO;2.
- Bolton, D., 1980: The computation of equivalent potential temperature. *Mon. Wea. Rev.*, **108**, 1046–1053, doi:10.1175/1520-0493(1980)108<1046:TCOEPT>2.0.CO;2.
- Brubaker, K. L., and D. Entekhabi, 1995: An analytic approach to modeling land–atmosphere interaction: 1. Construct and

- equilibrium behavior. *Water Resour. Res.*, **31**, 619–632, doi:[10.1029/94WR01772](https://doi.org/10.1029/94WR01772).
- Byrne, M. P., and P. A. O’Gorman, 2013a: Land–ocean warming contrast over a wide range of climates: Convective quasi-equilibrium theory and idealized simulations. *J. Climate*, **26**, 4000–4016, doi:[10.1175/JCLI-D-12-00262.1](https://doi.org/10.1175/JCLI-D-12-00262.1).
- , and —, 2013b: Link between land–ocean warming contrast and surface relative humidities in simulations with coupled climate models. *Geophys. Res. Lett.*, **40**, 5223–5227, doi:[10.1002/grl.50971](https://doi.org/10.1002/grl.50971).
- , and —, 2015: The response of precipitation minus evapotranspiration to climate warming: Why the “wet-get-wetter, dry-get-drier” scaling does not hold over land. *J. Climate*, **28**, 8078–8092, doi:[10.1175/JCLI-D-15-0369.1](https://doi.org/10.1175/JCLI-D-15-0369.1).
- Cao, L., G. Bala, K. Caldeira, R. Nemani, and G. Ban-Weiss, 2010: Importance of carbon dioxide physiological forcing to future climate change. *Proc. Natl. Acad. Sci. USA*, **107**, 9513–9518, doi:[10.1073/pnas.0913000107](https://doi.org/10.1073/pnas.0913000107).
- Chadwick, R., I. Boutle, and G. Martin, 2013: Spatial patterns of precipitation change in CMIP5: Why the rich do not get richer in the tropics. *J. Climate*, **26**, 3803–3822, doi:[10.1175/JCLI-D-12-00543.1](https://doi.org/10.1175/JCLI-D-12-00543.1).
- , P. Good, and K. M. Willett, 2016: A simple moisture advection model of specific humidity change over land in response to SST warming. *J. Climate*, **29**, 7613–7632, doi:[10.1175/JCLI-D-16-0241.1](https://doi.org/10.1175/JCLI-D-16-0241.1).
- Collins, M., and Coauthors, 2013: Long-term climate change: Projections, commitments and irreversibility. *Climate Change 2013: The Physical Science Basis*, T. F. Stocker et al., Eds., Cambridge University Press, 1029–1136.
- Cronin, T. W., 2013: A sensitivity theory for the equilibrium boundary layer over land. *J. Adv. Model. Earth Syst.*, **5**, 764–784, doi:[10.1002/jame.20048](https://doi.org/10.1002/jame.20048).
- Dai, A., 2006: Recent climatology, variability, and trends in global surface humidity. *J. Climate*, **19**, 3589–3606, doi:[10.1175/JCLI3816.1](https://doi.org/10.1175/JCLI3816.1).
- De Jeu, R. A. M., W. Wagner, T. R. H. Holmes, A. J. Dolman, N. C. Van De Giesen, and J. Friesen, 2008: Global soil moisture patterns observed by space borne microwave radiometers and scatterometers. *Surv. Geophys.*, **29**, 399–420, doi:[10.1007/s10712-008-9044-0](https://doi.org/10.1007/s10712-008-9044-0).
- Frierson, D. M. W., 2007: The dynamics of idealized convection schemes and their effect on the zonally averaged tropical circulation. *J. Atmos. Sci.*, **64**, 1959–1976, doi:[10.1175/JAS3935.1](https://doi.org/10.1175/JAS3935.1).
- , I. M. Held, and P. Zurita-Gotor, 2006: A gray-radiation aquaplanet moist GCM. Part I: Static stability and eddy scale. *J. Atmos. Sci.*, **63**, 2548–2566, doi:[10.1175/JAS3753.1](https://doi.org/10.1175/JAS3753.1).
- Fu, Q., and S. Feng, 2014: Responses of terrestrial aridity to global warming. *J. Geophys. Res. Atmos.*, **119**, 7863–7875, doi:[10.1002/2014JD021608](https://doi.org/10.1002/2014JD021608).
- Held, I. M., and B. J. Soden, 2000: Water vapor feedback and global warming. *Annu. Rev. Environ. Energy*, **25**, 441–475, doi:[10.1146/annurev.energy.25.1.441](https://doi.org/10.1146/annurev.energy.25.1.441).
- , and —, 2006: Robust responses of the hydrological cycle to global warming. *J. Climate*, **19**, 5686–5699, doi:[10.1175/JCLI3990.1](https://doi.org/10.1175/JCLI3990.1).
- Joshi, M. M., J. M. Gregory, M. J. Webb, D. M. H. Sexton, and T. C. Johns, 2008: Mechanisms for the land/sea warming contrast exhibited by simulations of climate change. *Climate Dyn.*, **30**, 455–465, doi:[10.1007/s00382-007-0306-1](https://doi.org/10.1007/s00382-007-0306-1).
- Lainé, A., H. Nakamura, K. Nishii, and T. Miyasaka, 2014: A diagnostic study of future evaporation changes projected in CMIP5 climate models. *Climate Dyn.*, **42**, 2745–2761, doi:[10.1007/s00382-014-2087-7](https://doi.org/10.1007/s00382-014-2087-7).
- Manabe, S., 1969: Climate and the ocean circulation. *Mon. Wea. Rev.*, **97**, 739–774, doi:[10.1175/1520-0493\(1969\)097<0739:CATOC>2.3.CO;2](https://doi.org/10.1175/1520-0493(1969)097<0739:CATOC>2.3.CO;2).
- , R. J. Stouffer, M. J. Spelman, and K. Bryan, 1991: Transient responses of a coupled ocean–atmosphere model to gradual changes of atmospheric CO₂. Part I: Annual mean response. *J. Climate*, **4**, 785–818, doi:[10.1175/1520-0442\(1991\)004<0785:TROACO>2.0.CO;2](https://doi.org/10.1175/1520-0442(1991)004<0785:TROACO>2.0.CO;2).
- O’Gorman, P. A., 2012: Sensitivity of tropical precipitation extremes to climate change. *Nat. Geosci.*, **5**, 697–700, doi:[10.1038/ngeo1568](https://doi.org/10.1038/ngeo1568).
- , and T. Schneider, 2008: The hydrological cycle over a wide range of climates simulated with an idealized GCM. *J. Climate*, **21**, 5797–5806, doi:[10.1175/2008JCLI2099.1](https://doi.org/10.1175/2008JCLI2099.1).
- , and C. J. Muller, 2010: How closely do changes in surface and column water vapor follow Clausius–Clapeyron scaling in climate change simulations? *Environ. Res. Lett.*, **5**, 025207, doi:[10.1088/1748-9326/5/2/025207](https://doi.org/10.1088/1748-9326/5/2/025207).
- Piao, S., P. Friedlingstein, P. Ciais, N. de Noblet-Ducoudré, D. Labat, and S. Zaehle, 2007: Changes in climate and land use have a larger direct impact than rising CO₂ on global river runoff trends. *Proc. Natl. Acad. Sci. USA*, **104**, 15 242–15 247, doi:[10.1073/pnas.0707213104](https://doi.org/10.1073/pnas.0707213104).
- Richter, I., and S.-P. Xie, 2008: Muted precipitation increase in global warming simulations: A surface evaporation perspective. *J. Geophys. Res.*, **113**, D24118, doi:[10.1029/2008JD010561](https://doi.org/10.1029/2008JD010561).
- Rowell, D. P., and R. G. Jones, 2006: Causes and uncertainty of future summer drying over Europe. *Climate Dyn.*, **27**, 281–299, doi:[10.1007/s00382-006-0125-9](https://doi.org/10.1007/s00382-006-0125-9).
- Santer, B. D., and Coauthors, 2005: Amplification of surface temperature trends and variability in the tropical atmosphere. *Science*, **309**, 1551–1556, doi:[10.1126/science.1114867](https://doi.org/10.1126/science.1114867).
- Schneider, T., P. A. O’Gorman, and X. J. Levine, 2010: Water vapor and the dynamics of climate changes. *Rev. Geophys.*, **48**, RG3001, doi:[10.1029/2009RG000302](https://doi.org/10.1029/2009RG000302).
- Sellers, P. J., and Coauthors, 1996: Comparison of radiative and physiological effects of doubled atmospheric CO₂ on climate. *Science*, **271**, 1402–1405, doi:[10.1126/science.271.5254.1402](https://doi.org/10.1126/science.271.5254.1402).
- Seneviratne, S. I., T. Corti, E. L. Davin, M. Hirschi, E. B. Jaeger, I. Lehner, B. Orlowsky, and A. J. Teuling, 2010: Investigating soil moisture–climate interactions in a changing climate: A review. *Earth-Sci. Rev.*, **99**, 125–161, doi:[10.1016/j.earscirev.2010.02.004](https://doi.org/10.1016/j.earscirev.2010.02.004).
- , and Coauthors, 2013: Impact of soil moisture–climate feedbacks on CMIP5 projections: First results from the GLACE-CMIP5 experiment. *Geophys. Res. Lett.*, **40**, 5212–5217, doi:[10.1002/grl.50956](https://doi.org/10.1002/grl.50956).
- Sherwood, S. C., and M. Huber, 2010: An adaptability limit to climate change due to heat stress. *Proc. Natl. Acad. Sci. USA*, **107**, 9552–9555, doi:[10.1073/pnas.0913352107](https://doi.org/10.1073/pnas.0913352107).
- , and Q. Fu, 2014: A drier future? *Science*, **343**, 737–739, doi:[10.1126/science.1247620](https://doi.org/10.1126/science.1247620).
- Simmons, A. J., K. M. Willett, P. D. Jones, P. W. Thorne, and D. P. Dee, 2010: Low-frequency variations in surface atmospheric humidity, temperature, and precipitation: Inferences from reanalyses and monthly gridded observational data sets. *J. Geophys. Res.*, **115**, D01110, doi:[10.1029/2009JD012442](https://doi.org/10.1029/2009JD012442).
- Sutton, R. T., B. Dong, and J. M. Gregory, 2007: Land/sea warming ratio in response to climate change: IPCC AR4 model results

- and comparison with observations. *Geophys. Res. Lett.*, **34**, L02701, doi:[10.1029/2006GL028164](https://doi.org/10.1029/2006GL028164).
- Taylor, K. E., R. J. Stouffer, and G. A. Meehl, 2012: An overview of CMIP5 and the experiment design. *Bull. Amer. Meteor. Soc.*, **93**, 485–498, doi:[10.1175/BAMS-D-11-00094.1](https://doi.org/10.1175/BAMS-D-11-00094.1).
- Vecchi, G. A., and B. J. Soden, 2007: Global warming and the weakening of the tropical circulation. *J. Climate*, **20**, 4316–4340, doi:[10.1175/JCLI4258.1](https://doi.org/10.1175/JCLI4258.1).
- Willett, K. M., P. D. Jones, N. P. Gillett, and P. W. Thorne, 2008: Recent changes in surface humidity: Development of the HadCRUH dataset. *J. Climate*, **21**, 5364–5383, doi:[10.1175/2008JCLI2274.1](https://doi.org/10.1175/2008JCLI2274.1).
- , R. J. H. Dunn, P. W. Thorne, S. Bell, M. De Podesta, D. E. Parker, P. D. Jones, and C. N. Williams Jr., 2014: HadISDH land surface multi-variable humidity and temperature record for climate monitoring. *Climate Past*, **10**, 1983–2006, doi:[10.5194/cp-10-1983-2014](https://doi.org/10.5194/cp-10-1983-2014).
- , D. I. Berry, and A. J. Simmons, 2015: Surface humidity [in “State of the Climate in 2014”]. *Bull. Amer. Meteor. Soc.*, **96** (12), S20–S22.